ISSN 1060-992X, Optical Memory and Neural Networks, 2023, Vol. 32, No. 3, pp. 204–218. © Allerton Press, Inc., 2023.

Optimization of Metamaterial Unit Cell Using Radial Basis Function Neural Network

Shilpa Srivastava[a], *, Sanjay Kumar Singh[a], **, and Usha Tiwari[a], ***

[a] *Department of Electronics and Communication, ABES Engineering College, Ghaziabad, 201009 India*

**e-mail: s.srivastava.ece@gmail.com*

***e-mail: ssinghraj@yahoo.com*

****e-mail: usha.tiwri@sharda.ac.in*

Received June 14, 2023; revised July 6, 2023; accepted July 7, 2023

Abstract—Microstrip Patch Antennas (MPA) are being used more and more in current communication systems because of their advantages such as being Lightweight, easy to construct, and low cost. However, MPA operational bandwidth and power handling capabilities are restricted. In this research, a novel unit cell MPA is designed and optimized using a Radial Basis Function Neural network (RBFNN). Flame-retardant (FR4) metamaterial is used in the fabrication of the envisioned antenna and the device. The High-Frequency Structure Simulator (HFSS) version 15 software is used for the design and simulation of the model. The design is simulated at a frequency range of 2 to 6 Hertz. Finally, the implementation of the antenna is performed using Complementary Split Ring Resonator (CSRR) technique. The proposed structure produces an excellent reflection coefficient, and Voltage Standing Wave Ratio (VSWR), which are −15.12 at 1.5 GHz, −55.41 at 2.5 GHz, and −25.63 dB at 3.5 GHz and 2.0 dB respectively. Simulation results show an excellent outcome, as return losses are 23.18, 38.67, and 44.12 dB at 0.6, 1.7, and 3.5 GHz respectively, and the gain is 8.5 dB at 6 GHz, which are quite similar to the actual values. The proposed unit cell antenna outperformed the other previously designed microstrip antenna and is suitable for wireless communication systems.

Keywords: Microstrip Patch antenna (MPA), FR4 metamaterial, return loss, passivity, CSRR technique

DOI: 10.3103/S1060992X23030098

1. INTRODUCTION

Antenna designers have shown a significant amount of interest in composite routine structures like Electromagnetic Bandgap (EBG) and Metamaterials (MTM) throughout the past few years. This interest can be attributed to the exceptional physical properties and innovative technologies of these composite structures [1, 2]. Microstrip Patch Antennas (MPA) have been the antenna technology that has had the greatest rate of advancement over the last fifteen years. It has attracted the imaginative consideration of scholars from all over the globe, and as a result, several patents, reports, and books have been written on them. As a direct consequence of this, microwave phased arrays have rapidly progressed from being an academic curiosity to a widely used component in commercial microwave systems [3]. Figure 1 shows the illustration of an MPA.

Typical MPAs consist of a patch on one side of a dielectric substrate and a ground plane on the other. In comparison to other antenna systems, MPAs have a low profile, are lightweight, and are straightforward to combine with Monolithic Microwave Integrated Circuits (MMICs) [5, 6].

1.1. Metamaterial (MTM)

"Meta" is a Greek word that means "something beyond", "altered", "transmuted", or "something advanced", and "material" is a term that was created by combining "meta" with "material" [7]. Incipient artificial materials, also known as MTM, have Electrical and Magnetic (EM) characteristics that cannot be found in naturally existing substances. The term "betokens metamaterials" refers to man-made structures that are engineered to have features that cannot be found in nature [8]. Figure 2 shows the characterization of MTM based on permeability.

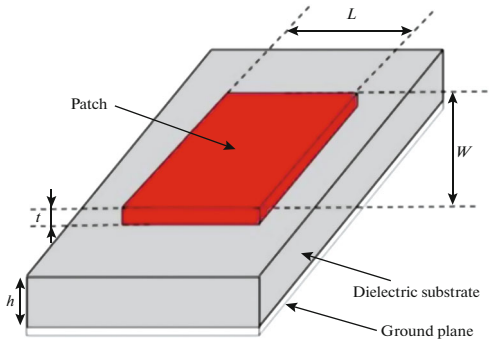

Fig. 1. Geometry of an MPA [4].

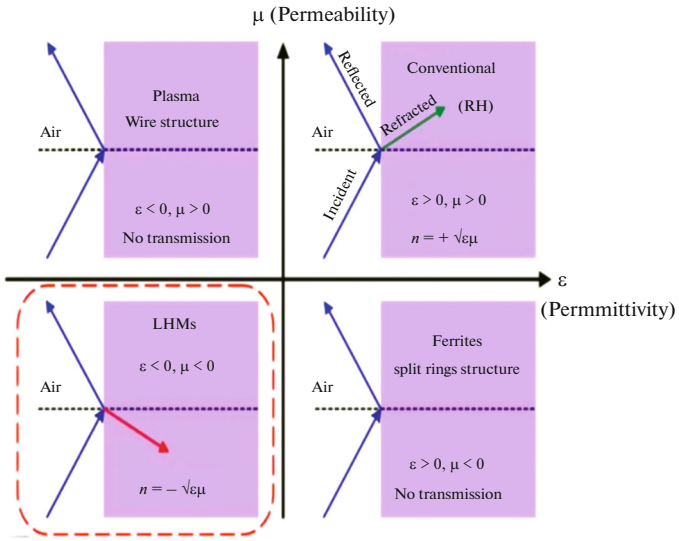

Fig. 2. Characterization of MTM [9].

The electrical permittivity, magnetic permeability, and index of refraction of natural materials are all positive. On the other hand, it is negative for all MTM. MTMs have been given the names negative index materials, double negative media, left-handed materials, and backward wave media because they have all negative values for these characteristics [10, 11]. For the wireless communication and military sectors, these MTMs would allow for the creation of new kinds of microwave components and devices, in addition to tiny antennas [12].

1.2. Role of MTM in Patch Antenna

Numerous researchers are working toward the goal of improving the performance of microwave, wireless telecommunications, nanoelectronics, and optical inventions by making use of these emerging MTMs [13]. It might be possible to increase the power that is emitted by the antenna by applying MTM [14]. The primary properties of MTM, such as negative permeability and permittivity can be employed in the production of electrically tiny antennas that are highly directional and capable of being reconfigured [15]. These antennas are also able to display enhanced efficiency, higher bandwidth capability, and an improvement in the beam scanning reach of antenna arrays [16]. Figure 3 shows the diagram of the patch antenna with the MTM substrate.

Some applications of MTM in patch antenna are as follows:

• These antennas aid with a variety of systems, including navigation systems, communication linkages, surveillance sensors, and command and control systems.

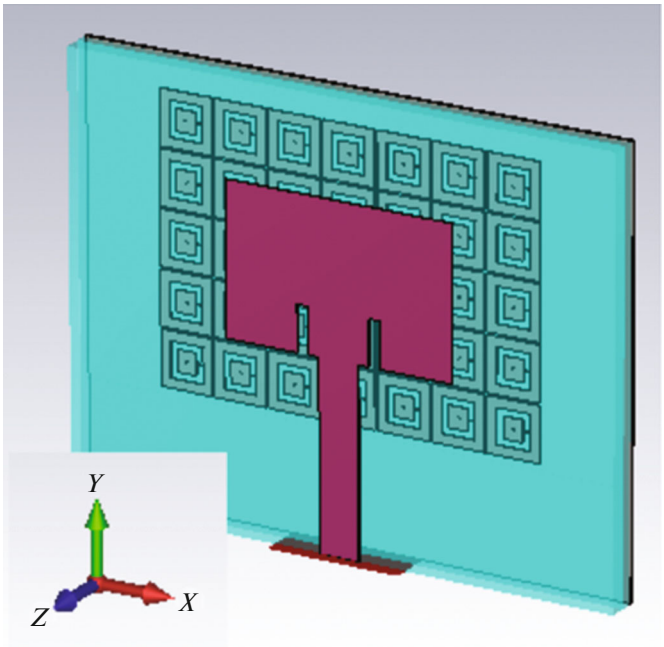

Fig. 3. MTM substrate-filled patch antenna [2].

• For aircraft applications using nanocomposites employing MTM technology, the emitted light is blocked and regulated by broad angles [17].

• Thin film technology that has been enhanced using MTM nanocomposites is being used to increase the performance of solar cells by collecting light from broad angles and collecting it throughout the spectrum of significance.

• The use of the MTM lens has contributed to improvements in the MPA's gain, as well as its efficiency and bandwidth [18].

2. LITERATURE REVIEW

This section displays multiple similar works by several writers based on the MPA.

Zhou et al. [19] synthesized MgF2 ceramics by using the conventional solid-state reaction process, and for the first time, the microwave dielectric characteristics of these ceramics were reported. When sintered at a temperature of 1100 deg, a material reaches its maximum potential for microwave dielectric characteristics. With a return loss of 23.39 dB and an impedance range of 318 MHz, the MgF2-based antenna that resonates at 8.25 GHz demonstrates remarkable antenna efficiency.

Kinagi et al. [20] showed a patch antenna that could operate on three distinct frequencies simultaneously. After being simulated with the help of mentor graphics software, the antennas are put through their paces utilizing a Vector Network Analyzer (VNA). In the end, it concluded that the variation in width was responsible for the correct impedance matching, which led to a gain that was more than 0 dB throughout all of the bands of operation.

Hossain et al. [21] presented a simple MPA that, by using a positive-intrinsic-negative diode, can reorient their polarization states in real-time such that they could switch from linear to circular polarization. To simulate the antenna, an Advanced Design System (ADS) simulation was utilized. It displays the minimal reflection coefficient increase with a –10 dB scattering bandwidth (100 MHz for linear polarization levels and 170 MHz for circular polarization states).

Mohan et al. [22] proposed a simple, cost-effective, and space-saving triangular microstrip antenna incorporating MTM. Its intended use was for cordless sensor node applications. The suggested microstrip antenna has a patch in the form of a triangle, and the ground plane is a Split Ring Resonator (SRR) in a circular configuration. The relationship between the measured and simulated reflection coefficients of the planned triangular antenna was derived by utilizing the VNA as an analytical tool. In the end, researchers

Table 1. Comparison of the reviewed literature

Author Name	Techniques	Outcomes
Zhou et al., (2023) [19]	Solid-state reaction method	The MgF2-based 8.25 GHz antenna performs well compared to other models
Kinagi et al., (2023) [20]	VNA	The width shift ensures good impedance matching and a gain larger than 0 dB in all bands
Hossain et al., (2023) [21]	ADS	It displays minimal reflection coefficient gain at 100 MHz for linear polarization states and 170 MHz for circular polarization states with a −10 dB scattering bandwidth
Mohan et al., (2022) [22]	VNA	The 2.4 GHz ISM band coverage makes the antenna suitable for WSN operations
Ahmed et al., (2022) [23]	MTM inclusion method	Compared to a λ/2 MPA, the zeroth-order resonant antenna reduces by 64%
Ali et al., (2022) [24]	5-G technology	The antenna's gain values are larger than 4 dB and all characteristics are below −10
Khaleel et al., (2022) [25]	3D full-wave software	The double-face superstrate MTM improves antenna performance and provides additional resonant frequency that might be employed in 6G communications
Sagik et al., (2021) [26]	Artificial neural network	MPA-MTM interactions boost antenna gain and directivity

concluded that the transmitter covers the 2.4 GHz band, which makes it suitable for use in Wireless Sensor Network (WSN) applications.

Ahmed et al. [23] developed a space-saving arrangement for a zeroth-order resonator antenna that had improved bandwidth. Utilizing the MTM inclusion technique allows for a reduction in the overall dimension of the zeroth-order resonator antenna. In the end, researchers concluded that the suggested zeroth-order resonant antenna achieves a 64% decrease in energy usage in comparison to a conventional λ/2 MPA.

Ali et al. [24] developed a fifth generation (5G) 3.5 GHz 22 Multiple Input and Multiple Output (MIMO) antennae. The antenna's layout is derived from a prior design; however, the backdrop and patch size have been modified to improve performance. When all characteristics are below −10 and gains are larger than 4 dB, as was predicted, it could be concluded that the antenna has performed as intended.

Khaleel et al. [25] found that graphene patch antennas are often utilized in telecommunications. On a Flame Retardant (FR4) substrate, a rectangular multi-pole antenna based on graphene is created. Two different commercial 3D full-wave programs are utilized to develop and optimize the recommended antenna. An additional resonant frequency is created by the double-face superstrate MTM, which could be utilized in future 6G communications.

Sagik et al. [26] developed an MPA with built-in MTMs. Artificial neural networks are used to determine the optimal parameters for the antenna's frequency, gain, and directivity. As a consequence, when MPA and MTM components interact, the antenna's gain and directivity both increase. Table 1 shows the comparative analysis of the literature of review for different authors.

3. BACKGROUND STUDY

MPA offers numerous benefits, but it also has some major downsides. As a result of their resonant nature, patch antennas have a limited frequency range. Broadband applications using standard patch configurations are constrained by bandwidth by as little as a few percent. This work aims to enhance the characteristics of a W-shaped patch antenna used in wireless communication systems by loading it with a CSRR metamaterial. Using CSRR metamaterial, the suggested structure improves gain, bandwidth, and reflection coefficient by 5.9 dBi at 5.5 GHz, −27.56 dB at 6 GHz, −12.65 dB at 4 GHz, and −21.24 dB at 8 GHz, while also achieving the desired radiation pattern. Return losses are −13.61, −16.42, and −35.86 dB at 4.2, 6.2, and 8 GHz, and the gain is 7.1 dB at 6.2 GHz for the antenna loaded with a metamaterial [27].

4. PROBLEM FORMULATION

The utilization of microstrip antennas in modern communication systems is becoming increasingly common as a result of the various benefits that these antennas offer. Some of these benefits include being very lightweight, having a simple construction, and having inexpensive efficiency. However, microstrip antennas have several limitations, such as limited working bandwidth and poor power handling capacity; as a result, their application in wireless systems is restricted. The MPA also has the disadvantage of being susceptible to surface wave stimulation. Choosing the appropriate feeding mechanism, substrate width, and dielectric constant can help you address the problem. In this research, HFSS (version 15) is used for the designing and simulation process and FR4 MTM is used as a substrate for the fabrication process. The MTM is inserted using a CSRR on both sides of the antenna. FR4 MTM can decrease the number of losses, boost the gain, and focus the radiation by acting as a lens.

5. RESEARCH OBJECTIVES

- To design and create an MPA using MTM as the substrate for the MPA.
- To improve the characteristics of antennas used in wireless communication systems, such as their bandwidth and gain.
- To enhance the directivity of the MPA using MTM structures.

6. RESEARCH GAPS

- Utilizing liquid MTM loading is one method that can be used to further increase the efficiency of MPA.
- Furthermore, an MPA with significant gain and a customized waveform can be utilized for wireless communication applications operating on the C-band and X-band frequencies.
- To further improve the performance of the antenna system, the antenna has been loaded with two layers of passive superstrate patches, which have been layered one on top of the other.

7. RESEARCH METHODOLOGY

The concept of designed architecture is examined in the context of research methodology. With the help of HFSS, the antenna is modeled and tested virtually. RBFNN method is used to optimize the result further the FR4 MTM is implemented by using the CSRR technique.

7.1. Technique Used

Two techniques are used in the proposed methodology. These techniques are stated below:

7.1.1. Complementary Split Ring Resonator (CSRR) method. The MTM is implemented by the CSRR method on both sides of the antenna. The CSRR's Resonant Frequency is determined by:

$$\omega_0 = \frac{1}{\sqrt{L_c C_c}}, \tag{1}$$

$$L_c = \frac{4.86}{2}\mu_0 (L - w - s)\left[\ln\left(\frac{0.98}{\rho} + 1.84\rho\right)\right], \tag{2}$$

$$\rho = \frac{w + s}{L - w - s}, \tag{3}$$

$$C_c = \left(L - 1.5(2 + d)C_{\text{pul}}\right), \tag{4}$$

where ρ is the filling factor, s is the outer ring, C_{pul} is the capacitance per unit, C_c is capacitance, w is width, l is length and L_c is impedance [28].

7.1.2. Radial Basis Function Neural Network (RBFNN). A feedforward NN is an RBFNN that offers a faster learning rate and a more integrated structure than other networks. The input layer, output layer, and hidden layer are the three layers that make up RBFNN. The Gaussian activation function is chosen because of its ability and differentiability to build a non-linear connection [29]. The Gaussian activation function $\varphi_i(x)$ is represented by the following equation:

$$\varphi_i(x) = e^{\frac{\left\|\sum_{j=1}^{N} w' jix_{j-c_i}\right\|^2}{2\sigma_i^2}}. \quad (5)$$

7.2. Proposed Methodology

Figure 4 depicts the proposed methodology in flowchart form. The methodology of the proposed model is completed in 7 steps:

7.2.1. Following are the steps of the proposed methodology.

Step 1: Design the geometrical dimension of the MPA. At the beginning of the process first, the designing parameters for the antenna consisting of the patch have been defined through the use of computing dimension. The geometrical parameters such as length L, width w, and substrate thickness s, are taken into consideration while designing the antenna. The following equation is taken into consideration while calculating L, W, and h:

$$h \geq \frac{0.06\lambda}{\sqrt{\varepsilon_r}}, \quad (6)$$

$$w = \frac{c}{2f_0}\frac{\sqrt{2}}{\varepsilon_{r+1}}, \quad (7)$$

$$L = \frac{c}{2f_{0\sqrt{\epsilon_r}}}, \quad (8)$$

where ε_r is permittivity, f_0 is frequency, and λ is the wavelength.

Step 2: Optimization of dimension. After designing the geometrical dimension of the MPA the next step is to optimize the dimension of the antenna. The optimization of dimension is an important step because it helps the antenna to achieve compact size and convenience in installation.

Step 3: Design and simulation in HFSS. In step 3, HFSS (version 15) software is used for the design and simulation of the model. It has been determined that the design under consideration operates at a frequency of 6 GHz. The frequency is calculated using below equation:

$$f_0 = \frac{c}{\lambda}, \quad (9)$$

where c is the speed of light.

Step 4: Result optimization using RBFNN. After the designing and simulation of the antenna in this step the optimization of the result using RBFNN is performed. The input layer, output layer, and hidden layer are the three layers that make up RBFNN.

Step 5: Evaluate the optimized result. After the designing and simulation of the antenna in this step, the optimization of the result is evaluated. If the result is obtained after the simulation is not optimized then again, the process starts from step 2 and if the results are optimized, then the methodology proceeds further.

Step 6: MTM selection. In step 5, the FR4 MTM is used as the substrate for the fabrication process. The FR4 has a relative permittivity of 4 and a thickness of 1.6 mm. An antenna with a high dielectric substrate would be smaller in size due to the inverse relationship between the antenna's size and its dielectric constant.

Step 7: Evaluating performance parameters. After the fabrication process of the MPA in the last step, the parameters are evaluated such as the Reflection coefficient, gain, and bandwidth to check the performance of the designed MPA.

8. DESIGNING OF MPA WITH FR4 SUBSTRATE AND WITHOUT FR4 SUBSTRATE

In this section, the design of unit cell MPA using an FR4 substrate is discussed in detail. With the help of HFSS (version 15), the antenna is modeled and tested virtually and operates at a frequency of 6 GHz. In the process of creating a microstrip patch antenna, a metal layer known as a feed wire or transmission

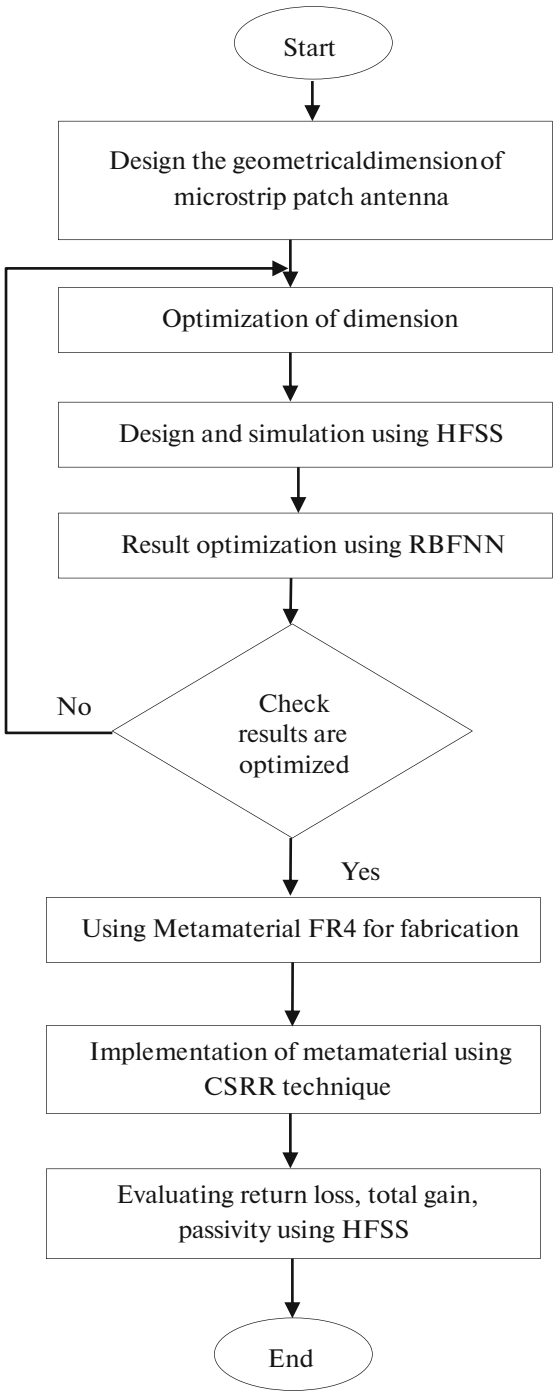

Fig. 4. Block diagram of the proposed framework.

line is utilized. This layer is responsible for feeding the patch antenna frequency and allowing the wavelengths to be sent to the ground plane. Through the use of the feed wire, a connection can be made between the patch antenna and the ground plane. The patch has a length of L and a width of W, and it is positioned on the surface of the substrate or the insulating circuit board, which has a thickness of h. Figure 5a shows the design of MPA having FR4 metamaterial as a substrate and Fig. 5b shows the MPA design without FR4 metamaterial as a substrate. Figure 6a shows the back side of unit cell MPA, Fig. 6b shows the front side of unit cell MPA Fig. 6c depicts the enlarged image of the back side of unit cell MPA.

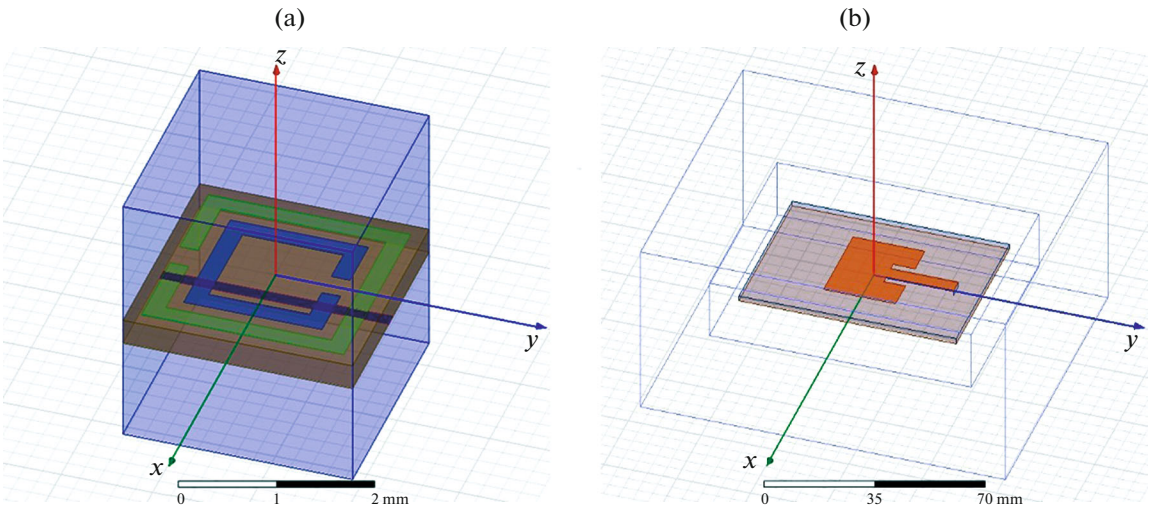

Fig. 5. Microstrip patch antenna with FR4 and without FR4 metamaterial.

9. RESULT AND DISCUSSION

In this section, various results of the proposed MPA design are presented with the help of computer simulation technology. MPA with FR4 metamaterial design model implementation is presented in the research work by using HFSS software (version 15). The proposed model is investigating various parameters such as total gain, directivity, passivity, return loss, VSWR, and many more in detail.

9.1. Result 1

In this numerical analysis, the total gain of unit cell MPA is investigated at a frequency range of 6 GHz. The peak radiation intensity is used to determine the gain of an antenna, which is a measurement of the antenna's ability to turn the input energy into radiation in a certain direction. The total gain of the MPA with FR4 substrate is 8.5 dB, as shown in the graph in Fig. 6.

9.2. Result 2

In this numerical analysis, the return loss of unit cell MPA is investigated at a frequency range of 6 GHz. It is a parameter that measures how much power goes wasted by the load and doesn't get reflected. Numerical analysis shows that the return loss is 23.18, 38.67, and 44.12 dB at 0.6, 1.7, and 3.5 GHz which can be seen in Fig. 8.

9.3. Result 3

In this numerical analysis, the reflection coefficient and directivity of the proposed unit cell MPA are investigated at a frequency range of 2 to 6 GHz. Figure 9 shows the reflection coefficient of the proposed antenna concerning the frequency range of 2 to 6. The reflection coefficient is a parameter that specifies the amount of a wave that is returned by an impedance irregularity in the medium through which the wave is transmitted, and numerical analysis shows that the reflection coefficient of the proposed unit cell MPA is −15.12, −55.41, and −25.63 dB, at 2.5, 3.5, and 1.5 GHz respectively. Directivity refers to the degree to which the radiation is focused in the location of the highest intensity. Numerical analysis shows that the directivity of the proposed unit cell MPA is 0615e+000 as shown in Fig. 10.

9.4. Result 4

In this numerical analysis, the passivity of unit cell MPA is investigated at a frequency range of 6 GHz. A system's passivity index quantifies the passivity gap between its supply and demand. When it is more than the number 1, it demonstrates positive behavior in terms of stability, however, when it is less than 1, it demonstrates a loss in terms of the stability parameter.

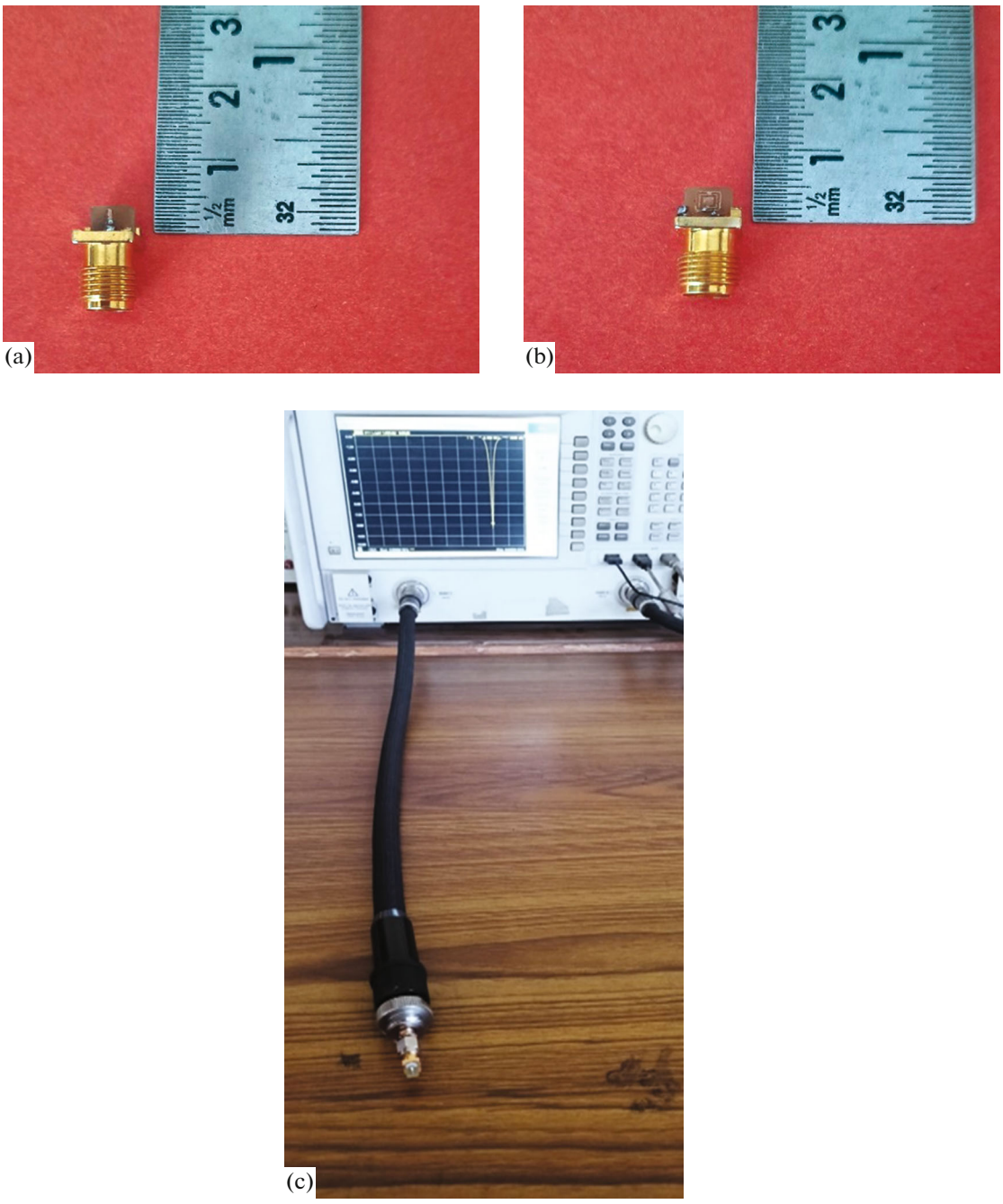

Fig. 6. Design of metamaterial loaded antenna and investigation of its characteristic using network analyzer. (a) Back side of unit cell MPA; (b) front side of unit cell MPA; (c) network analyzer.

9.5. Result 5

From Fig. 11, At 2.5 GHz, the antenna has an excellent impedance match, as the VSWR is 2.0. The ideal VSWR is less than 1.5 : 1. A VSWR of 2 : 1 is marginally acceptable in low-power scenarios where power loss is more significant. nevertheless, a VSWR of up to 6 : 1 can be used with the appropriate equipment.

9.6. Result 6

In this numerical analysis, various parameters of the antenna are discussed such as realized gain total, rE total, and axial ratio value. The graph of these parameters is shown in Fig. 13. Figure 13a shows the

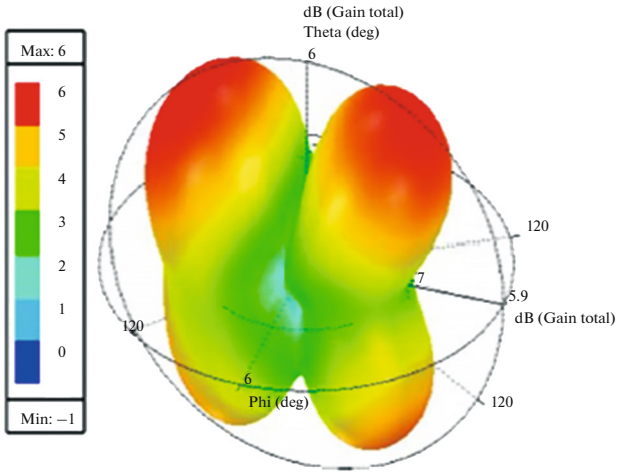

Fig. 7. Total gain (dB) vs. frequency.

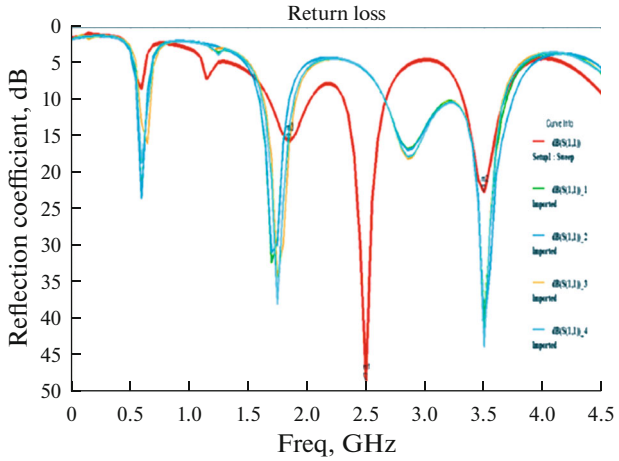

Fig. 8. Return loss vs. frequency.

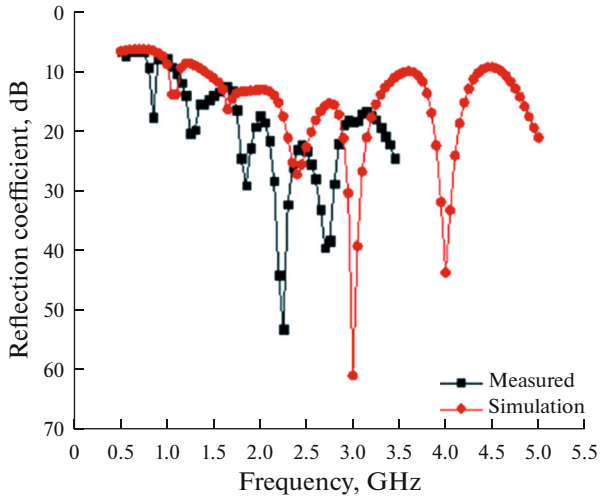

Fig. 9. Reflection coefficient (dB) vs. Frequency.

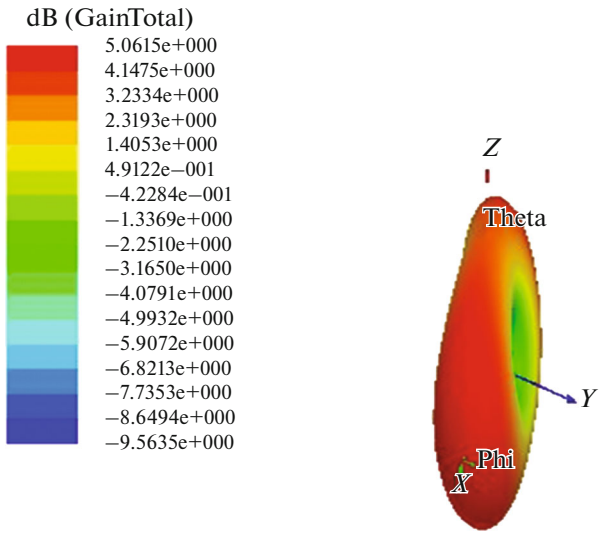

Fig. 10. 3D Radiation pattern of the proposed antenna.

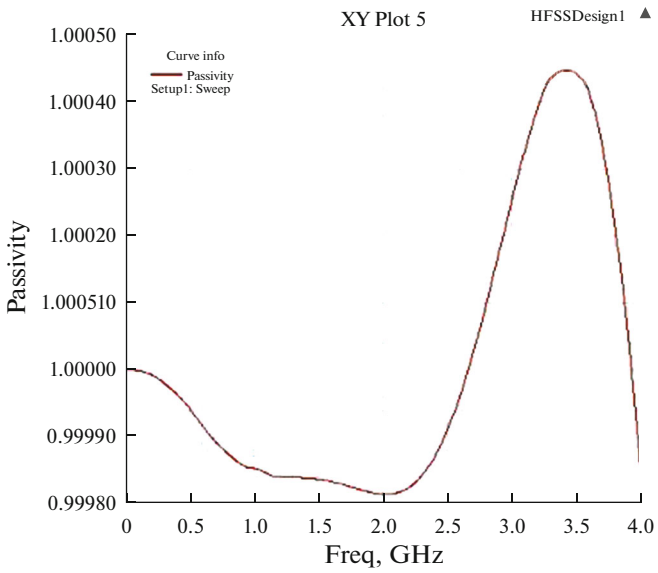

Fig. 11. Passivity.

radiation pattern of the realized gain total, Fig. 13b shows the radiation pattern of the rE total, and Fig. 13c shows the radiation pattern of the Axial ratio value.

• *Comparative analysis*

In this part, a comparison study between the proposed unit cell MPA and other established models is carried out. Several characteristics, including total gain, VSWR, return loss, and bandwidth, are used to make comparisons between the antennas as shown in fig. 14. The results of the numerical analysis are shown in Table 2, which includes both the numerical values of the suggested antenna and those of the other conventional model.

In Fig. 14a the comparison is performed based on gain total and the proposed antenna obtained the highest gain total (8.5 dB) among all the designed antennae, In Fig. 14b the comparison is performed based on bandwidth and the proposed antenna obtained the highest bandwidth (6.9 dB) among all the designed antenna, In Fig. 14c the comparison is performed based on return loss and the proposed antenna

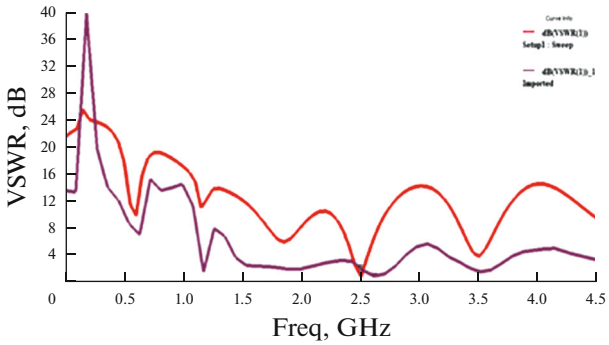

Fig. 12. VSWR vs. frequency plot for the substrate.

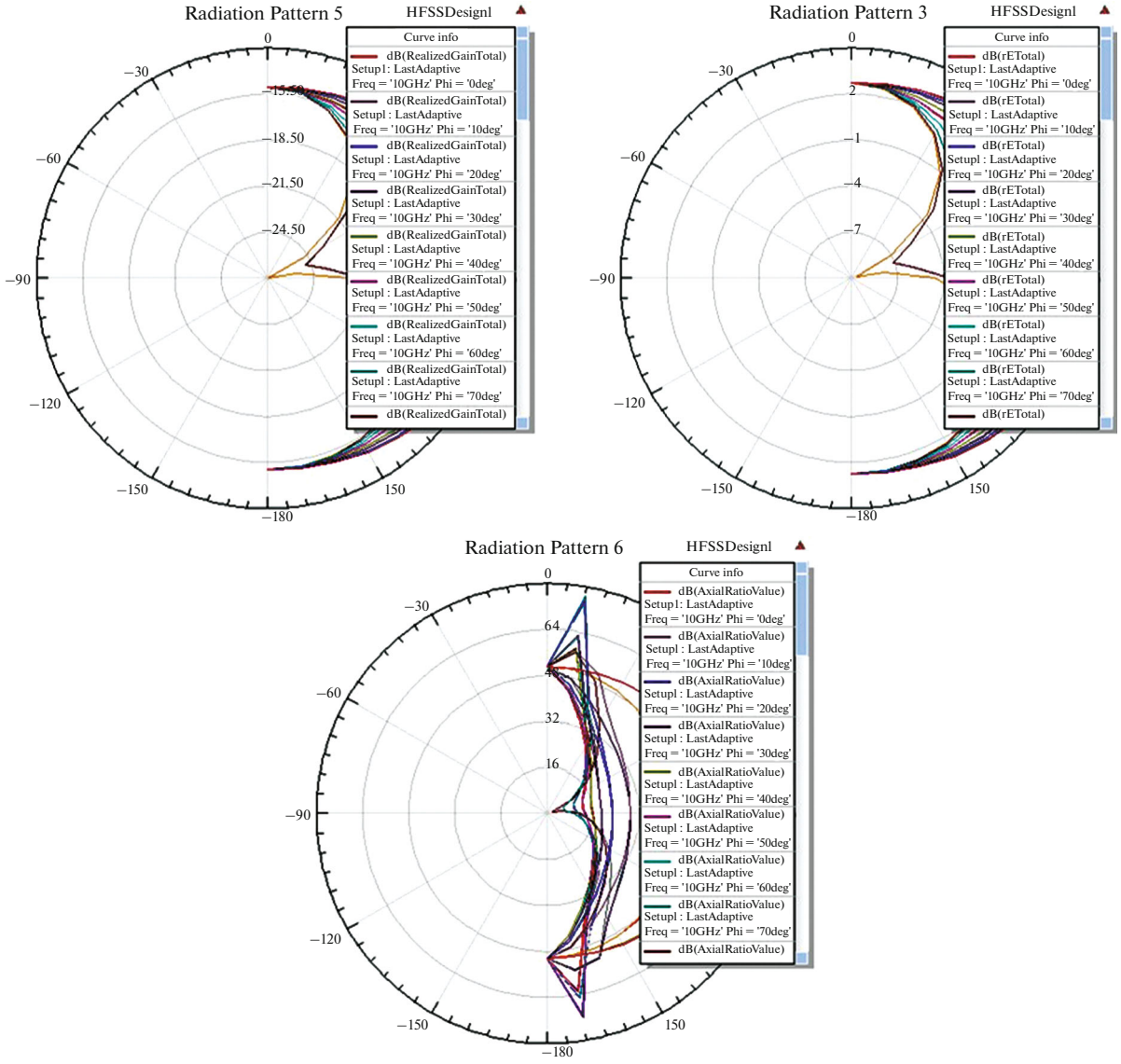

Fig. 13. Radiation pattern of the antenna.

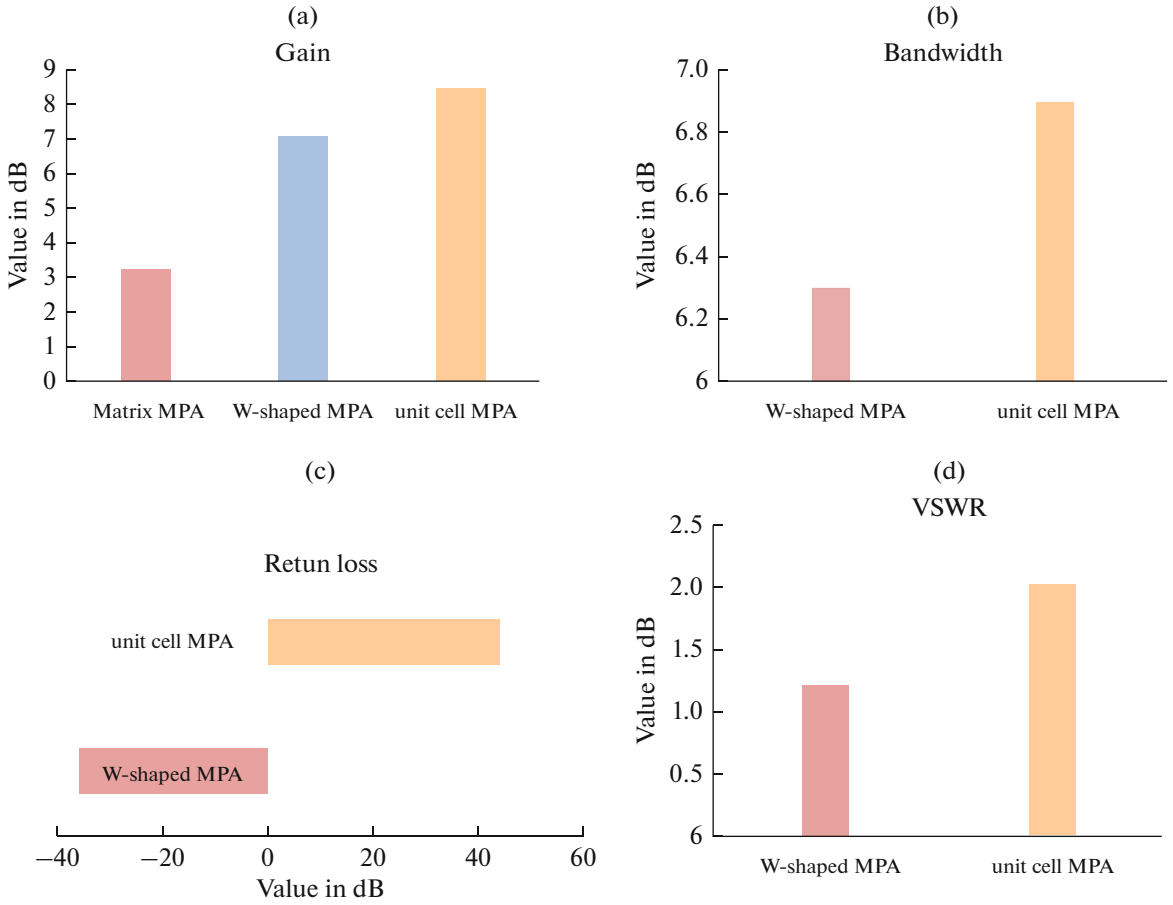

Fig. 14. Comparison of the proposed work's performance to that of similar current schemes in terms of (a) Total gain (b) Bandwidth (c) Return loss (d) VSWR.

obtained the highest return loss 44.12 dB) among all the designed antenna negative sign represent the direction of the loss, In Fig. 14d the comparison is performed based on VSWR and the proposed antenna obtained the highest VSWR (2.0 dB) among all the designed antenna.

Table 2. Comparative analysis of proposed antenna with previously designed antenna

Parameters	Proposed antenna	W-shaped patch antenna	5 × 5 Matrix patch antenna
Size, mm	0.5 ×0.5	30 ×30	30 ×40
metamaterial	FR4	FR4	FR4
Impedance, Ohm	50	50	50
Reflection coefficient	−15.12 dB @ 1.5 GHz, −55.41 @ 2.5 GHz, −25.63 dB @ 3.5 GHz	−13.61 @ 4.2 GHz, −35.86 @ 6.2 GHz, and −16.42 @ 8 GHz	−26 dB @ 2.4 GHz
Gain, dB	8.5	7.1	3.23
VSWR, dB	2.0	1.2	200MHz
Bandwidth, dB	6.9	6.3	–
Frequency (6–8)	6	6 and 8	2.4
Return loss	44.12	−35.86	–

10. CONCLUSIONS

The benefits of MPA, including portability, simplicity of build, and cheap cost, have led to their widespread use in modern communication systems. But MPAs have limited operating bandwidth and power handling capacities. This study employs an RBFNN and HFSS to develop and optimize a unique unit cell MPA. The suggested antenna is made using FR4 MTM. Modeling and simulation work is done in HFSS version 15. The design is tested in a frequency range from 2 to 6 Hz in the simulation. The CSRR technology is used to fabricate the antenna. Excellent reflection coefficients and VSWRs of –15.12 at 1.5 GHz, –55.41 at 2.5 GHz, and –25.63 dB at 3.5 GHz are generated by the suggested design. Also, in each case Gain is 8.5 dB at 6 GHz and return loss is 23.18 dB at 0.6 GHz, 38.67 dB at 1.7 GHz, and 44.12 dB at 3.5 GHz, all of which are quite close to the observed values. For wireless communication systems, the suggested unit cell antenna has shown to be more effective than any previously constructed microstrip antenna. In the future, antennas configured with array components have the potential to improve bandwidth, return loss, and gain.

CONFLICT OF INTEREST

The authors declare that they have no conflicts of interest.

REFERENCES

1. Anand Kumar and Dinesh Kumar V., High-performance metamaterial patch antenna, *Microwave Opt. Technol. Lett.,* 2013, vol. 55, no. 2, pp. 409–413.
2. Anand Kumar, Jitendra Mohan, and Hari Om Gupta, Microstrip patch antenna loaded with metamaterial for multiband applications, *International Conference on Signal Processing and Communication (ICSC)*, IEEE, 2016, pp. 43–47.
3. Anand Kumar, Dinesh Kumar, Jitendra Mohan, and Hari Om Gupta, Investigation of grid metamaterial and EBG structures and its application to patch antenna, *Int. J. Microwave Wireless Technol.*, 2015, vol. 7, no. 6, pp. 705–712.
4. Kaur Harmandeep and Sharma Aditi, Microstrip patch antennas using metamaterials: A review, *Int. J. Electron., Electr. Comput. Syst.,* 2017, vol. 6, no. 6, pp. 130–133.
5. Bansal Aakash and Gupta Richa, A review on microstrip patch antenna and feeding techniques, *Int. J. Inf. Technol.,* 2020, vol. 12, no. 1, pp. 149–154.
6. Khan Muhammad Umar, Mohammad Said Sharawi, and Mittra Raj, Microstrip patch antenna miniaturization techniques: A review, *IET, Microwaves, Antennas Propagation*, 2015, vol. 9, no. 9, pp. 913–922.
7. Baviskar Jaypal, Mullay Afshan, and Jeyakumarz Amutha, erformance analysis of uniform meta-material lens embedded patch antennas, *IEEE International Symposium on Antennas and Propagation and USNC/URSI National Radio Science Meeting*, IEEE, 2015, pp. 1914–1915.
8. Baviskar Jaypal, Mulla Afshan, Baviskar Amol, Auti Dinesh, and Waghmare Rohit, Performance enhancement of microstrip patch antenna array with the incorporation of metamaterial lens, *IEEE Aerospace Conference*, IEEE, 2016, pp. 1–10.
9. Imtiaz Masudul Haider and Hashmi Galib, Towards high-efficiency solar cells: Composite metamaterials, *Global J. Res. Eng.,* 2013, vol. 13, no. F10, pp. 11–16.
10. Wu Wenwang, Wenxia Hu, Guian Qian, Liao Haitao, Xu Xiaoying, and Berto Filippo, Mechanical design and multifunctional applications of chiral mechanical metamaterials: A review, *Mater. Design,* 2019, vol. 180, p. 107950.
11. Yu Xianglong, Ji Zhou, Liang Haiyi, Jiang Zhengyi, and Wu Lingling, Mechanical metamaterials associated with stiffness, rigidity, and compressibility: A brief review, *Progress Mater. Sci.,* 2018, vol. 94, pp. 114–173.
12. Zadpoor Amir, A., Mechanical meta-materials, *Mater. Horiz.,* 2016, vol. 3, no. 5, pp. 371–381.
13. Ajay, V.G., and Mathew Thomaskutty, Size reduction of microstrip patch antenna through metamaterial approach for WiMAX application, *International Conference on Wireless Communications, Signal Processing and Networking (WiSPNET)*, IEEE, 2017, pp. 379–381.
14. Jain Satish K., Shrivastava Ayush, and Shrivas Gautam, Miniaturization of microstrip patch antenna using metamaterial loaded with SRR, in *2015 International Conference on Electromagnetics in Advanced Applications (ICEAA)*, IEEE, 2015, pp. 1224–1227.
15. Shelton, D.J., Brener Igal, Ginn, J.C., Sinclair, M.B., Peters, D.W., Coffey, K.R., and Boreman, G.D, Strong coupling between nanoscale metamaterials and phonons, *Nano Lett.,* 2011, vol. 11, no. 5, pp. 2104–2108.
16. Farooq Bushra, Parveen Tahira, Ali Imad, and Ullah Sadiq, Antenna design for advance wireless systems using metamaterial surfaces, *13th International Bhurban Conference on Applied Sciences and Technology (IBCAST)*, IEEE, 2016, pp. 641–646.

17. Baviskar Jaypal, Mulla Afshan, Baviskar Amol, and Pawar Sandeep, Metamaterial lens incorporated enhanced gain omnidirectional conformal patch antenna, *IEEE Aerospace Conference*, IEEE, 2016, pp. 1–7.
18. Dewan, R., Rahim, M.K.A., Hamid, M.R., Samsuri, N.A., and Bala, B.D., Analysis of triple band artificial magnetic conductor (AMC) band conditions to wideband antenna performance, *IEEE Asia-Pacific Conference on Applied Electromagnetics (APACE)*, IEEE, 2014, pp. 167–170.
19. Zhou Meng Fei, Liu Bing, Chao Hu Cheng, and Song Kai Xin, Ultra-low permittivity MgF_2 ceramics with high Qf values and their role as microstrip patch antenna substrates, *Ceram. Int.*, 2023, vol. 49, no. 1, pp. 369–374.
20. Revansiddappa, S.K., Ravi M. Yadahalli, and Siddarama R. Patil, A novel microstrip fed triple band patch antenna with TM10, TM02, and TM12 induced modes, *Bull. Electr. Eng. Inf.,* 2023, vol. 12, no. 2, pp. 800–806.
21. Hossain Md Azad, Rahman Muhammad Asad, Murshed Abu Hena, Eisuke Nishiyama, and Toyoda Ichihiko, A simple design and fabrication of polarization reconfigurable antenna for industrial scientific and medical-band applications, *Int. J. Electr. Comput. Eng. (IJECE),* 2023, vol. 13, no. 2, pp. 1580–1587.
22. Mohan Chinnasamy and Sundarsingh Esther Florence, Miniaturised triangular microstrip antenna with metamaterial for wireless sensor node applications, *IETE J. Res.,* 2022, vol. 68, no. 2, pp. 1177–1182.
23. Ahmed Sadiq, Zaid A. Abdul Hassain, Hussein A. Abdulnabi, and Al-Saadi Mohammed, Design and bandwidth enhancement of zeroth-order resonator antenna using metamaterial, *TELKOMNIKA (Telecommunication Computing Electronics and Control),* 2022, vol. 20, no. 3, pp. 494–500.
24. Ali Faris, Salih Maithem, and Ilyas Muhammad, MIMO Patch Antenna with Metamaterial 3.5 GHz for 5G Applications, *2nd International Conference on Advances in Electrical, Computing, Communication and Sustainable Technologies (ICAECT)*, IEEE, 2022, pp. 1–4.
25. Khaleel, S.A., Hamad, E.K.I., and Saleh, M.B., High-performance tri-band graphene plasmonic microstrip patch antenna using superstrate double-face metamaterial for THz communications, *J. Electr. Eng.,* 2022, vol. 73, no. 4, pp. 226–236.
26. Sağık Metin, Altıntaş Olcay, Ünal Emin, Özdemir Ersin, Demirci Mustafa, Çolak Şule, and Karaaslan Muharrem, Optimizing the gain and directivity of a microstrip antenna with metamaterial structures by using an artificial neural network approach, *Wireless Personal Commun.,* 2021, vol. 118, no. 1, pp. 109–124.
27. Ananda Babu Devarapalli and Tamasi Moyra, Design of a metamaterial loaded W-shaped patch antenna with FSS for improved bandwidth and gain, *Silicon*, 2022, vol. 15, no. 3, pp. 1–14.
28. Kai Yu, Yingsong Li, and Yanyan Wang, Multi-band metamaterial-based microstrip antenna for WLAN and WiMAX applications, *International Applied Computational Electromagnetics Society Symposium-Italy (ACES)*, IEEE, 2017, pp. 1–2.
29. Shymkovych, V., Telenyk S., and Kravets, P., Hardware implementation of radial-basis neural networks with Gaussian activation functions on FPGA, *Neural Comput. Appl.,* 2021, vol. 33, no. 15, pp. 9467–9479.